# Barometer Measurement Error Modeling and Correction for UAH Altitude Tracking

Xue Bao[1], Zhi Xiong[1], Shouzhao Sheng[1], Yijie Dai[1], Sheng Bao[1], Jianye Liu[1]

1. College of Automation Engineering, Nanjing University of Aeronautics & Astronautics, Nanjing 210016, China
E-mail: bxue@nuaa.edu.cn

**Abstract:** Altitude is a significant flight parameter for Unmanned Aerial Helicopters(UAH). Traditional vertical damping loop has been used to improve stability of vertical channel of the INS(inertial navigation system) with auxiliary altitude information. Barometer is a common and popular altimeter which can provide the continuous and reliable altitude information, however the measurement performance is rather poor due to several factors, including principle error, drifting behavior and sensitivity to environment changes in pressure uncorrelated with altitude. In this paper, the characteristics of the barometer measurement errors have been thoroughly investigated and we decomposed the barometer measurement errors into three components: principle error, drift error and external disturbance error. We proposed a scheme to estimate and correct the barometer measurement errors. GPS has been utilized in this paper as an auxiliary altimeter. A method has been proposed to estimate and correct the drift error by introducing a factor to change the measurement noise covariance. A serial experiments have been performed to validate the accuracy of the models and illustrate that the proposed method has better performance than normal Kalman filter.

**Key Words:** Barometer, Measurement error model, Correction, Kalman filter

## 1 INTRODUCTION

Altitude information is important for autonomous flight control of UAHs. Inertial navigation systems are self-contained, dead-reckoning navigation systems with inertial measurement units (IMUs) [1], widely used in UAHs. However, the shortcoming of an INS is the instability in the vertical channel [2]. Conventionally, inertial navigation systems with vertical damping loop have been used in dealing with the problem. This damping loop mixes the vertical acceleration measurements and reference altitude to produce stable altitude information through the complimentary filter structure [3]. Since the major error characteristics of the system are determined by the reference altitude error properties, it has been a major issue how to construct an accurate reference altitude providing system viz. reference altitude generator [4].

To cope with this problem, auxiliary altimeters such as GPS, Lidar, ultrasonic range finder are frequently adopted nowadays. However, these sensors have not shown satisfactory performance in many adverse conditions such as large roll attitude of the vehicle and various jamming environments. As one of the most popular reference altitude generator, barometers have been commonly used which derive altitude from pressure measurements. In general, barometers are initialized with the altitude, temperature, and pressure at the starting point of the UAH where the barometer is installed. A barometer sensor is orientation independent and can provide altitude measurements continuously. Unfortunately, barometers have drifting behavior problems with time elapses. In addition, the characteristics of the atmosphere around the UAH are changed when the UAH moves to another place, resulting in large barometer principle error. Furthermore, pressure altitude is susceptible to external disturbance such as airflow and vibration. Consequently, it is required to compensate these errors to provide the INS vertical channel with stable accurate altitude reference. In [5], a stochastic approach was developed to barometric altimeter noise modeling and the barometric altimeter noise is assumed to be the additive combination of a deterministic time-varying mean, an exponentially time-corrected random process and an uncorrected random process.

Although other auxiliary altimeters have their own shortcomings, we can still utilize their altitude measurements to correct or to be integrated with barometer measurements. A new reference height generator using baro-error identification/compensation to steadily supply the accurate baro-altitude was presented in [4]. A method of intercalibration for GPS and high precision baro-altimeter on line was proposed in [6]. In [7], heave estimation method using time differenced GPS carrier phase measurement and compensated barometer measurement applying error model was proposed.

In this paper, we mainly state the characteristics of the barometer measurement errors and decompose the er-

This work was partially supported by the National Natural Science Foundation of China (Grant No. 61533008, 61673208, 61533009, 61374115), the "333 project" in Jiangsu Province (Grant No. BRA2016405), the Scientific Research Foundation for the Selected Returned Overseas Chinese Scholars(Grant No. 2016), the peak of six personnel in Jiangsu Province (Grant No. 2013-JY-013), the Fundamental Research Funds for the Central Universities(Grant No. NZ2016104), Foundation of Jiangsu Key Laboratory "Internet of Things and Control Technologies" & the Priority Academic Program Development of Jiangsu Higher Education Institutions.

978-1-5090-4657-7/17/$31.00 ©2017 IEEE

rors into three components: principle error, drift error and external disturbance error, together with the error modeling. The barometer altitude information is combined with the GPS altitude information by Kalman filter to estimate and correct the drift error. Since the positioning accuracy of GPS is unstable, we proposed a method that introduces a factor to properly change the measurement noise covariance according to the positioning accuracy of GPS, which can improve the estimation accuracy. Experiments are performed for demonstrating the accuracy of the models and the effectiveness of the proposed method.

## 2 BAROMETER MEASUREMENT ERROR MODELING

The barometer measurement performance is affected by several noise source including principle error, drift error, external disturbance error, and sensor error. The sensor error is out of the scope of this paper. In this paper, the error $\delta_h^{baro}$ superimposed to the output of a barometer is assumed to be the additive combination of three different components:

$$\delta_h^{baro} = \varepsilon_p + \varepsilon_d + \varepsilon_e \tag{1}$$

where $\varepsilon_p$ is the principle error, $\varepsilon_d$ is the drift error and $\varepsilon_e$ is the external disturbance error.

### 2.1 PRINCIPLE ERROR

As is well-known, the atmospheric pressure is a physical property strongly related with the altitude above a certain level. Barometric sensors are used to sense the value of the pressure and then transform the pressure to the altitude by Equation (2).

$$H_p = H_0 - \frac{T_0}{\beta}\left[1 - \left(\frac{P}{P_0}\right)^{-\frac{\beta R}{g}}\right] \tag{2}$$

In the equation, $H_0$, $T_0$, $P_0$ are the altitude, temperature, and pressure at the initial point respectively, $R$ is the universal gas constant, $\beta$ is the lapse rate, $g$ is the gravity constant. The composition of the lower atmosphere is approximately constant, but in a very wet atmosphere the water vapor content can be high enough to significantly lower the density of the air, thus changing the value of $R$. The lapse rate is defined as the rate of temperature increase in the atmosphere with the altitude: a constant lapse rate $L$ can be assumed between 0 and 11 km $(L = -6.5K/km)$ – the negative sign indicates that the temperature decreases with altitude. The assumption of constant gravity is not crucial in solving Equation (2), that is, the variation of gravity with altitude and latitude can be safely ignored for short-distance trips [8].

As UAH moves, the current atmospheric condition is different from the initial point atmospheric condition. Thus, the actual pressure $P_0^{'}$ and temperature $T_0^{'}$ are disagree with $T_0$ and $P_0$ respectively, resulting in principle errors.

Let $H = f(P_0^{'}, T_0^{'})$, carrying out Taylor expansion of $H$ at the point $(P_0, T_0)$, we obtain the Equation (3).

$$\begin{aligned} & f\left(P_0^{'}, T_0^{'}\right) = \\ & f(P_0,T_0) + \left(\Delta P\frac{\partial}{\partial P_0} + \Delta T\frac{\partial}{\partial T_0}\right) f(P_0,T_0) \\ & + \frac{1}{2!}\left(\Delta P\frac{\partial}{\partial P_0} + \Delta T\frac{\partial}{\partial T_0}\right)^2 f(P_0,T_0) + \cdots \\ & + \frac{1}{n!}\left(\Delta P\frac{\partial}{\partial P_0} + \Delta T\frac{\partial}{\partial T_0}\right)^n f(P_0,T_0) + O(\rho) \end{aligned} \tag{3}$$

In the equation, $\Delta P = P_0^{'} - P_0$, $\Delta T = T_0^{'} - T_0$ are the increment between actual sea level atmospheric parameters $P_0^{'}$, $T_0^{'}$ and standard sea level atmospheric parameters $P_0$, $T_0$. $O(\rho)$ is the remainder. Let $\Delta H = f(P_0^{'}, T_0^{'}) - f(P_0, T_0)$, when $\Delta P$ and $\Delta T$ are both small, the first-order Taylor expansion of $H$ at the point$(P_0, T_0)$ can meet the accuracy requirement as follows:

$$\begin{aligned} \Delta H &= \left(\Delta P\frac{\partial}{\partial P_0} + \Delta T\frac{\partial}{\partial T_0}\right) f(P_0,T_0) \\ &= \frac{T_0 R}{g P_0}\left(\frac{P_s}{P_0}\right)^{-\frac{\beta R}{g}} \cdot \Delta P + \frac{1}{\beta}\left(1 - \left(\frac{P_s}{P_0}\right)^{-\frac{\beta R}{g}}\right) \cdot \Delta T \\ &= \frac{R}{gP_0}(T_0 + H\beta)\cdot \Delta P + \frac{H}{T_0}\cdot \Delta T \end{aligned} \tag{4}$$

Thus, we can conclude that the principle error is mainly consist of a scale factor $a = \frac{R\beta}{g}\cdot\frac{\Delta P}{P_0} + \frac{\Delta T}{T_0}$ and a bias $b = \frac{RT_0}{g}\cdot\frac{\Delta P}{P_0}$ as shown in the formula (5) .

$$\varepsilon_p = a \cdot H + b \tag{5}$$

where $H$ is the true altitude.

### 2.2 DRIFT ERROR

Drift error is time-varying, correlated with slow pressure changes that can be involved in,e.g.,local weather forecasting and long-time tracking [9]. Drift behavior greatly affects the measurement performance of barometer, the top plot in Figure 1 shows that the barometric altitude drifts upward about 10 meters in an hour indoors without moving, the temperature in the room is almost constant. In general, the trend of the drift varies with the local weather, season and time. The drift error time series is non stationary, but the first order difference of the drift error time series is a white Gaussian stochastic process as shown in the bottom plot in Figure 1. Accordingly, the drift error $\varepsilon_d$ can be modeled as the following random walk process.

$$\dot{\varepsilon_d}(t) = w(t) \tag{6}$$

In the equation, $w(t)$ is a white Gaussian stochastic process with zero mean and variance $\sigma^2$. $\sigma^2$ is deeply dependent on the local weather, season and time.

### 2.3 EXTERNAL DISTURBANCE ERROR

Barometer measurements are susceptible to the external disturbance uncorrelated with altitude such as wind and vibration. In this paper, we mainly discussed the external

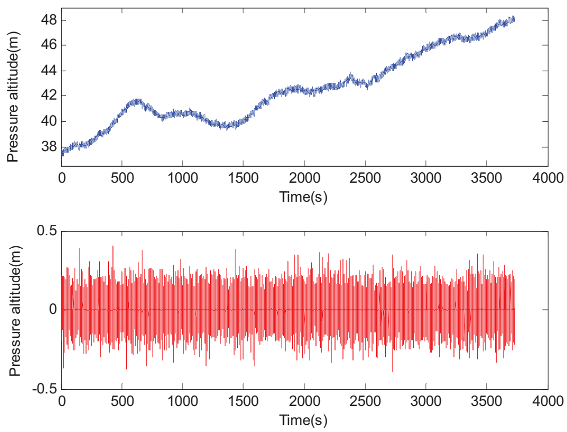


Figure 1: Pressure altitude recorded from the barometric altimeter(indoors static condition) and the pressure altitude after differential treatment

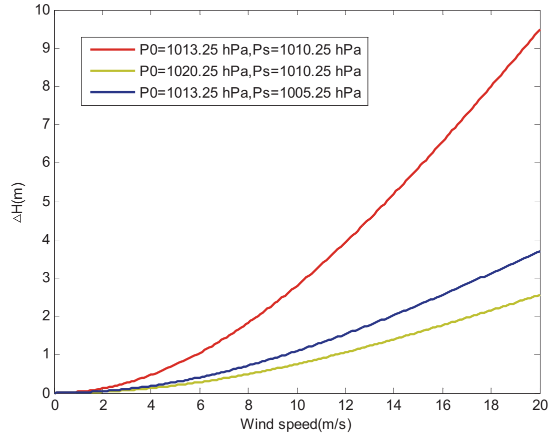


Figure 2: Curves describing the relationship between $\Delta H$ and wind speed.

disturbance error caused by wind. The occured wind will influence the air pressure around the UAH to produce an external disturbance error.

Since the total pressure is composed of the static pressure and the dynamic pressure, and the total pressure is constant, the increment in dynamic pressure caused by wind will result in the decrement in static pressure. The dynamic pressure can be calculated by the following formula:

$$P_D = \frac{1}{2}\rho v^2 \tag{7}$$

where $P_D$ is the dynamic pressure, $\rho = 1.25kg/m^3$ is the standard air density and $v$ is the speed of wind.

According to formula(2), the static pressure decreases with the pressure altitude. The disturbed static pressure $P_S^{'}$ and corresponding pressure altitude $H^{'}$ measured by the barometer can be described as follows:

$$P_S^{'} = P_S - \frac{1}{2}\rho v^2 \tag{8}$$

$$H^{'} = H_0 - \frac{T_0}{\beta}\left[1 - \left(\frac{P_S^{'}}{P_0}\right)^{-\frac{\beta R}{g}}\right] \tag{9}$$

The difference between $H^{'}$ and actual altitude $H$ is given by formula(10)

$$\begin{aligned} \Delta H &= H^{'} - H \\ &= \frac{T_0}{\beta}\left[\left(\frac{P_S^{'}}{P_0}\right)^{-\frac{\beta R}{g}} - \left(\frac{P_S}{P_0}\right)^{-\frac{\beta R}{g}}\right] \end{aligned} \tag{10}$$

Figure 2 shows the relationship between $\Delta H$ and wind speed. The curves reflect the sensitivity of the barometer output to the wind disturbance. When the initial pressure $P_0$ is constant, the curve will be more gentle with the decrease of $P_S$; when the $P_S$ is constant, the curve will be steeper with the decrease of $P_0$. Hence, we obtained the external disturbance error as follows:

$$\varepsilon_e = \frac{T_0}{\beta}\left[\left(\frac{P_S^{'}}{P_0}\right)^{-\frac{\beta R}{g}} - \left(\frac{P_S^{'} - \frac{1}{2}\rho v^2}{P_0}\right)^{-\frac{\beta R}{g}}\right] \tag{11}$$

where $P_S^{'}$ is the pressure measured by the barometer.

## 3 BAROMETER MEASUREMENT ERROR CORRECTION

Based on the models investigated in the previous chapter, a barometer measurement error correction scheme is introduced in this chapter. In the previous chapter, the barometer measurement errors can be thought to be mostly composed of principle error, drift error and external disturbance error. To provide the INS vertical channel with stable accurate altitude reference, we designed a scheme to correct these errors as shown in Figure 3.

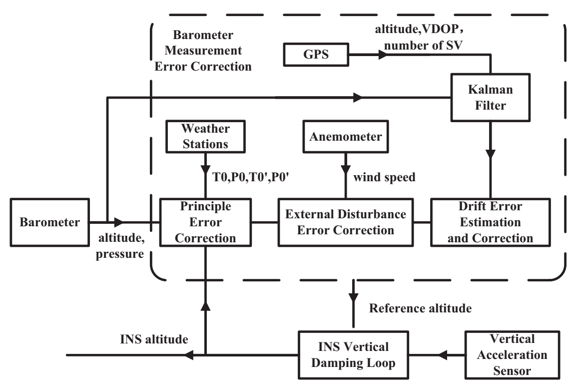


Figure 3: Barometer measurement error correction block diagram

### 3.1 PRINCIPLE ERROR CORRECTION

Principle error correction is very important in those applications where the absolute altitude is required. Based on Equation(5), the principle error correction value can be obtained with the scale factor $a$, the bias $b$ and the current true altitude $H$. Generally, the true altitude of the current time can not be obtained, thus, we use the altitude of the last time to replace $H$. The value of $a$ and $b$ can be calculated using the meteorological data provided by local weather stations. The atmospheric parameters of a certain place (such as an airport, etc.) with affirmatory altitude can be used to calculate the pressure and temperature of the actual sea level at this altitude. According to these parameters, the principle error can be calculated to correct the barometer measurements. In actual flight, the air temperature and pressure of the actual sea level have little change within a certain range, thus, it is not necessary to carry on the continuous correction to the principle error.

### 3.2 EXTERNAL DISTURBANCE ERROR CORRECTION

The external disturbance error correction requires the information of the interference source. The wind speed is needed to correct the external disturbance error caused by wind. Generally, the speed of wind can be measured by an anemometer or be solved by other sensors. When wind disturbance exists, the correction value of wind disturbance error can be obtained by taking the measured or calculated wind speed and current measured static pressure into formula(11). It is difficult to achieve real time correction of wind disturbance error in the actual flight, unless the wind and the wind speed can be predicted. If the accurate model of the wind field can be established, then the state of wind can be predicted to achieve a better performance of the wind disturbance error correction.

### 3.3 DRIFT ERROR CORRECTION

Kalman filter is an effective method to estimate the value of drift error $\varepsilon_d$. The observed quantity of the Kalman filter can be obtained by combining the barometer altitude information and other auxiliary altimeter altitude information. GPS is considered to provide the auxiliary altimeter altitude information in this paper. The top plot in Figure 4 shows the distinct characteristics of GPS relative altitude and barometer relative altitude in static condition. As we can see in the figure, the altitude provided by GPS is bumpier than the one derived from barometer. However, the GPS altitude error is not accumulated over time. The bottom plot in Figure 4 is the value of VDOP(Vertical Dilution of Precision) reflecting the vertical positioning accuracy of GPS. The smaller the value of VDOP, the higher the vertical positioning accuracy of GPS. Based on Equation(6), the discrete state dynamic model of filter in state-space form can be expressed as

$$\mathrm{X}(\mathrm{k}+1)=\mathrm{X}(\mathrm{k})+\mathrm{W}(\mathrm{k}) \tag{12}$$

where $\mathrm{W}(\mathrm{k})$ is the noise input vector with noise variance, $\mathrm{Q}(\mathrm{k})$. The state transition matrix $\mathrm{F}(\mathrm{k})$ and process noise transfer matrix $\mathrm{G}(\mathrm{k})$ are both equal to $[1]_{1\times1}$.

We take the difference between GPS altitude $\mathrm{H_G}$ and barometric altitude $\mathrm{H_B}$ as the observed quantity of the Kalman filter. We have the following corollary to the measurement equation: the altitude channel information of GPS can be expressed as: $\mathrm{H_G}=\mathrm{h_t}+\delta\mathrm{h_G}$, the altitude channel information of the barometer can be expressed as: $\mathrm{H_B}=\mathrm{h_t}-\delta\mathrm{h_B}$. Thus, $\mathrm{Z}=\mathrm{H_G}-\mathrm{H_B}=\delta\mathrm{h_B}+\delta\mathrm{h_G}$, the discrete observation model of filter in state-space form can be expressed as Equation(13)

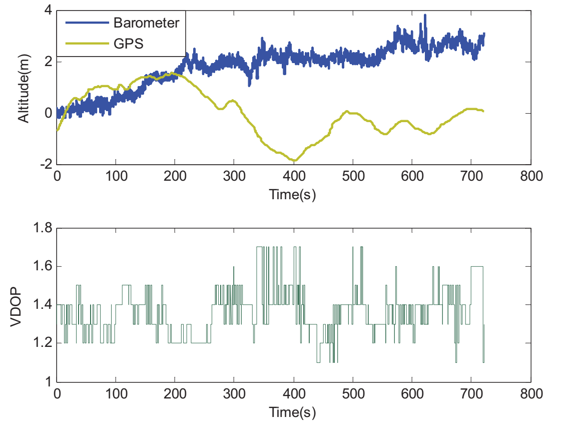


Figure 4: GPS relative altitude vs. barometric relative altitude and value of VDOP

$$\mathrm{Z}(\mathrm{k})=\mathrm{H}(\mathrm{k})\,\mathrm{X}(\mathrm{k})+\mathrm{V}(\mathrm{k}) \tag{13}$$

where $\mathrm{H}(\mathrm{k})=[1]_{1\times1}$, $\mathrm{V}(\mathrm{k})$ is the observation noise vector with noise variance, $\mathrm{R}(\mathrm{k})$. With these filter parameters, $\mathrm{F}(\mathrm{k})$, $\mathrm{G}(\mathrm{k})$, $\mathrm{H}(\mathrm{k})$, $\mathrm{R}(\mathrm{k})$ and the initial condition $\mathrm{P}(0)$, the Kalman filter can complete its estimation cycle.

Due to the effect of GPS satellite geometry, number of visible satellites, and multipath, GPS measurement noise will change. However, the observation noise covariance is changeless in the normal Kalman filter, so the tracking result is not good enough inevitably. Thus, in this paper, we proposed a method that introduces a factor $\eta$ to solve the degradation of the filter caused by GPS unstable measurement noise. The calculation of measurement noise covariance matrix $R$ is added to the normal Kalman filter. $R$ is weighted by $\eta$ as shown in Equation(14) and then influences the filter plus to overcome the instability of filter.

$$R_k=\eta_k\cdot C \tag{14}$$

In equation(14), $R_k$ and $\eta_k$ are the measurement noise covariance and the factor at $k$ moment respectively, $C$ is a constant depended on the worst vertical positioning accuracy of GPS. $0<\eta_k\leq1$, the greater the the $\eta_k$ is, the more unreliable GPS altitude information is. Since the effect of mutipath in flight is small, the value of $\eta$ is mainly dependent on the number of visible satellites and VDOP value.

## 4 EXPERIMENTS

### 4.1 HARDWARE SELECTION

To validate the models and our method, a number of commercially available devices were selected(Figure 5).

#### 4.1.1 BAROMETER SELECTION

A digital atmospheric pressure sensor MS5611 was chosen to obtain pressure value and temperature value. Ta-

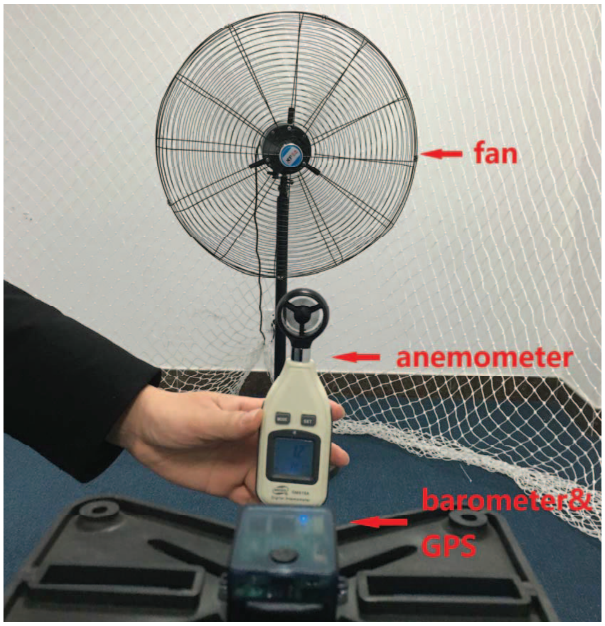


Figure 5: Experimental scene.

ble 1 shows the features of MS5611.

Table 1: MS5611 features.

| | |
|---|---|
| Pressure range | 10 hPa ~ 1200 hPa |
| High pressure resolution | 0.012 hPa |
| Altitude resolution | 10 cm |
| Temperature range | -40 ~ 85 $^{o}$C |
| Temperature Resolution | 0.01 $^{o}$C |
| Update rate | 10HZ |

#### 4.1.2 ANEMOMETER SELECTION

A digital anemometer GM816A was chosen to measure the speed and temperature of wind. Table 2 shows the features of GM816A.

Table 2: GM816A features.

| | |
|---|---|
| Wind speed range | 0 ~ 30 m/s |
| Wind speed resolution | 0.2 m/s |
| Wind temperature range | -10 ~ 45 $^{o}$C |
| Wind temperature resolution | 2 $^{o}$C |

#### 4.1.3 GPS RECEIVER SELECTION

The U-blox LEA-6H GPS receiver module was chosen as the auxiliary altimeter to provide information including altitude, value of VDOP and number of visible satellites. The update rate of the GPS receiver is 5 Hz.

### 4.2 WIND DISTURBANCE EXPERIMENTAL PROCEDURES AND RESULTS

In the experiments, a large electric fan was used to simulate the wind disturbance, the fan can generate wind with three different levels of wind speed. The speed of wind can be controlled by the fan gear and the distance between the barometer and the fan. The speed of wind can be obtained by GM816A. Two sets of experiments were carried out. In each set of experiments, the fan was used to simulate the wind with speed of 1.5m/s, 2.5m/s and 3.5m/s respectively. In each experiment, the barometer was motionless on a platform for about 1 minute firstly, and then we performed wind disturbance on it for about 1 minute. Since just the change of the measured pressure altitude was meaningful, only the relative pressure altitude was recored. The results of the first set experiments are shown in Figure 6.

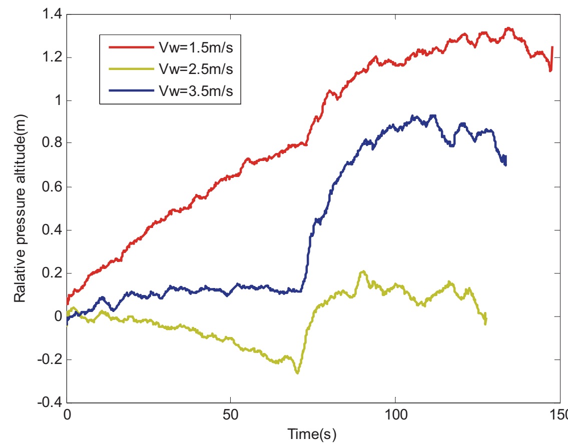


Figure 6: Results of first set experiments.

As we can see form Figure 6, when the wind disturbance occurs, the measured pressure altitude has an obvious change. Due to the instability of the wind field simulated by the fan and each experiment was carried out at different time in a same day, the long term trend of each curve is different. However, the trend of the change caused by wind disturbance is the same.

The two sets experiments results and corresponding theoretical results are presented in Table 3.

Table 3: Experimental values and theoretical values of barometer measurement errors caused by wind with different speed.

| $V_w$(m/s) | Set | Theoretical value(m) | Actual value(m) |
|---|---|---|---|
| 1.5 | 1 | 0.1283 | 0.2074 |
| | 2 | 0.1290 | 0.2328 |
| 2.5 | 1 | 0.3510 | 0.3693 |
| | 2 | 0.3512 | 0.3681 |
| 3.5 | 1 | 0.6857 | 0.7490 |
| | 2 | 0.6856 | 0.6458 |

The results are in good agreement with the comparable experimental and theoretical values. The correctness of the correction value calculated by the formula (11) is verified.

### 4.3 STATIC DRIFT EXPERIMENTAL PROCEDURES AND RESULTS

In the experiment, the barometer and GPS receiver were placed on a same certain altitude nearby. The experiment was carried out in an outdoor environment without wind, so the wind disturbance error can be ignored. Figure 7 shows the barometric altitude with only the drift error and the GPS altitude.

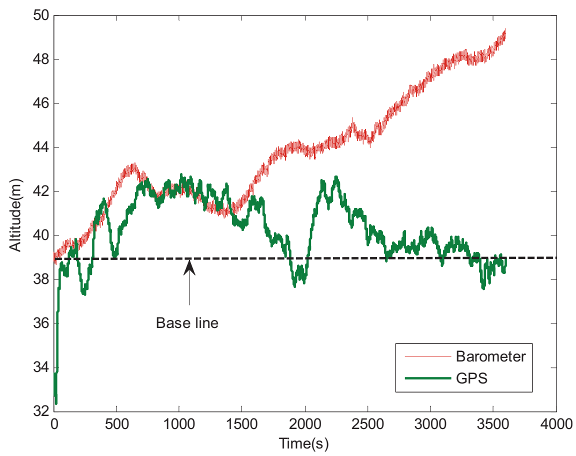


Figure 7: Barometric altitude and GPS altitude.

The normal Kalman filter and the proposed method were used to corrected the barometric altitude respectively, the results are shown in Figure 8.

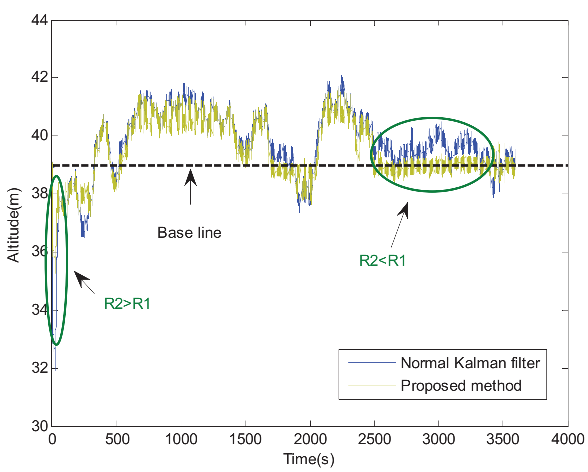


Figure 8: Barometric altitude corrected by normal Kalman filter and the proposed method.

In Figure 8, the black dashed line is the baseline of standard altitude. The barometric altitude corrected by the proposed method has smaller error than that one corrected by the normal Kalman filter, especially at the two places circled by the green ellipse. When the GPS has a poor accuracy, the proposed method will generate a larger measurement noise covariance $R$ as shown in the left green ellipse, and when the GPS has a good accuracy, the proposed method will generate a smaller $R$ as shown in the right green ellipse.

## 5 CONCLUSION

In this paper, the characteristics of the barometer measurement errors were analysed and the barometer measurement errors were decomposed into principle error, drift error and external disturbance error. The models of these errors were established respectively. A method was proposed to estimate and correct the drift error by introducing a factor to properly change the measurement noise covariance. GPS was utilized in this paper as an auxiliary altimeter. The experimental results demonstrate the accuracy of the models and the effectiveness of the proposed method.

## REFERENCES

[1] Nakanishi, H. and Kanata, S. and Sawaragi, T, GPS-INS-BARO hybrid navigation system taking into account ground effect for autonomous unmanned helicopter, IEEE International Symposium on Safety, Security, and Rescue Robotics, 1-6, 2012.

[2] Titterton, D. and Weston, J, T, Strapdown inertial navigation technology - 2nd edition, Aerospace & Electronic Systems Magazine IEEE, Vol.20, No.7, 33-34, 2005.

[3] Siouris, George M, Aerospace Avionics System: A Modern Synthesis, Academic Press, 1993.

[4] Whang, Ick Ho and Ra, Won Sang, Barometer error identification filter design using sigma point hypotheses, International Conference on Control, Automation and Systems, 1410-1415, 2007.

[5] Sabatini, Angelo Maria and Genovese, Vincenzo, A Stochastic Approach to Noise Modeling for Barometric Altimeters, Sensors, Vol.13, No.11, 15692-707, 2013.

[6] Gong, Xiao Lin, A Method of Intercalibration for GPS and High Precision Baro-Altimeter on Line, Dianzi Yu Xinxi Xuebao/journal of Electronics & Information Technology, Vol.31, No.4, 818-821, 2009.

[7] Lee, Dong Sun and Park, Kwi Woo and Park, Chansik and Kang, In Suk, An efficient heave estimation using Time-Differenced GPS carrier phase measurements and compensated barometer measurement applying error model, Navigation World Congress, 2015.

[8] Blanchard, R. L., A New Algorithm for Computing Inertial Altitude and Vertical Velocity, IEEE Transactions on Aerospace & Electronic Systems, Vol.7, No.6, 1143-1146, 1971.

[9] Seo, Jaewon and Lee, Jang Gyu and Chan, Gook Park, Bias suppression of GPS measurement in inertial navigation system vertical channel, Position Location and Navigation Symposium, 143-147, 2004. fig4